



Modelling the late-Holocene and future evolution of Monacobreen, northern Spitsbergen

Johannes Oerlemans¹

¹Institute for Marine and Atmospheric Research, Utrecht University, Princetonplein 5, Utrecht, 3585CC, The Netherlands

5 *Correspondence to:* Johannes Oerlemans (j.oerlemans@uu.nl)

Abstract. Monacobreen is a 40 km long surge-type tidewater glacier in northern Spitsbergen. The glacier flows down from Isachsenfonna (~1000 m a.s.l.), and drains an area of about 400 km². The longitudinal surface profile is smooth and the mean slope is small (0.027). During 1991-1997 Monacobreen surged and advanced by about 2 km, but the front did not reach the maximum LIA stand. Since 1997 the glacier front has receded over a distance of 2.5 km.

10 In this study Monacobreen is modelled with a Minimal Glacier Model, including a parameterization of the calving process as well as the effect of surges. The glacier is modelled as a 5 km wide flowband, to which 10 tributary glaciers and basins supply mass when they have a positive budget. The bed profile is not known, but supposed to be similar to that of Kronebreen, which flows from the same plateau into the opposite direction.

The model is driven by a well-constrained ELA history derived from lake sediments of a nearby glacier catchment (Røthe et al., 2015), in combination with meteorological data from 1899 onwards. The model is calibrated by optimising a surge parameter and the reference value of the ELA. The simulated glacier length is in good agreement with the observations: the maximum LIA stand, the front position at the end of the surge, and the 2.5 km retreat after the surge (1997-2016) are accurately reproduced.

15 The effect of surging, with a surge cycle of 100 years, appears to be limited. Directly after a surge the initiated mass-balance perturbation due to a lower mean surface elevation is about -0.16 m w.e./yr. This only has a modest effect on the long-term evolution of the glacier.

The simulation suggests that the major growth of Monacobreen after the Holocene Climatic Optimum started around 1500 BC. Monacobreen became a tidewater glacier around 500 BC, and reached a size comparable to the present state around 500 AD. After that the length of the glacier has fluctuated within a range of about 5 km. The e-folding time scale appears to be of the order of 350 years.

25 For the mid-B2 scenario (IPCC, 2013), which corresponds to a ~2 m/yr rise of the ELA, the model predicts a volume loss of 20 to 30 % by the year 2100 (relative to the 2017 volume). For a 4 m/yr rise in the ELA this is 30 to 40 %. However, much of the response to 21st century warming will come after 2100.

1 Introduction

30 In view of the observed strong warming of the polar regions, the future evolution of arctic ice masses is of great concern. Glacier retreat has a huge impact on regional ecosystems, and it contributes significantly to sea-level rise. The large ice sheets of Greenland and Antarctica are losing mass (IPCC, 2013; Van den Broeke et al., 2016; Martin-Español et al., 2017), and glaciers have retreated far behind their Little Ice Age maximum stands almost everywhere (Leclercq et al. 2014; Zemp et al., 2015). Even the large tidewater glaciers of the Arctic region have retreated over large distances (kilometers) during the past 100 years. Although tidewater and surging glaciers have a strong internal component to their dynamics, it has become clear that climatic forcing will now determine to a large extent their future evolution.



Different approaches have been taken to model the future behaviour of glaciers. Individual glaciers have been studied with flowline models based on approximate formulations of the mechanics of ice flow (e.g. Kruss, 1984; Huybrechts et al., 1989; Oerlemans, 1997; Nick et al., 2007). In more recent years, three-dimensional higher-order models have been employed, for instance for the Rhone glacier (Jouvet et al., 2009), and for the Morteratsch glacier (Zekkolari et al., 2013). Smaller ice caps are also being studied with such models (e.g. Zekkolari et al., 2017; Schäfer et al. (2015)).

The projection of future glacier changes depends very much on the definition of the initial state used to start the integration. Glaciers have response times of decades to centuries, implying that a reliable projection of future evolution can only be achieved when changes over a past timespan can first of all be reproduced (termed "dynamic calibration" in Oerlemans, 1997). This timespan should have a duration of at least the response time, preferably longer. In Oerlemans et al. (1998) this approach was applied to a sample of 12 glaciers, and a rather simple attempt was made to apply the results to the entire glacier population.

Along a different line, models have been constructed to treat the entire glacier population on the globe (e.g. Radic et al., 2014; Huss and Hock 2015). In these models the focus is on estimating global glacier mass changes as a response to warming and its effect on sea-level rise. Processes like accumulation, melting, calving and dynamic adjustments of glacier geometries are treated in a schematic way. The models have a large number of empirical parameters, and are tuned by comparison with observed mass balance data over the past decades. Clearly, when questions of a global nature have to be dealt with, global models are needed in which not every single glacier can be treated in detail. Nevertheless, it seems that in studies of this kind historical data on glacier fluctuations over the past centuries have not yet been fully exploited.

The modelling strategies discussed above have their advantages as well as their limitations. The 3-dimensional models require a large amount of geometric input data, and the issue of boundary conditions in steep terrain has not yet been resolved in a satisfactory way. There appears to be room for an intermediate approach with simpler models for individual glaciers that still take into account a number of essential feedback mechanisms (altitude-mass balance feedback, effect of overdeepenings, variable calving rates, effect of regular surging on the long-term mass budget, inclusion of tributary glaciers and basins).

Minimal Glacier Models (MGM's, Oerlemans 2011) offer the possibility to model individual glaciers in a relatively simple way, while still dealing with mechanisms like altitude - mass balance feedback, the effect of overdeepenings in the bed, variable calving rates, the effect of regular surging on the long-term mass budget, etc. MGMs hardly require computational resources (a 1000 year simulation takes a second on a standard laptop) and can therefore be used efficiently in control methods where many integrations have to be carried out. MGM's have been applied to MacGall glacier in Alaska, (Oerlemans, 2011), to Hansbreen, a calving glacier in southern Spitsbergen (Oerlemans et al., 2011), and to Abrahamsbreen, a surging glacier in northern Spitsbergen (Oerlemans and Van Pelt, 2015).

In this paper a MGM is applied to Monacobreen, a 40 km long glacier in northern Spitsbergen that flows from the plateau Isachsenfonna (~1000 m a.s.l.) into the Liefdefjord (glacier coordinates 79°23' N, 12°38' E; see the interactive topographic / thematic map operated by the Norsk Polarinstitutt: <http://toposvalbard.npolar.no>). The glacier drains an area of about 400 km², and the main stream has an average slope of only 0.027. Modelling Monacobreen is a real challenge, because it is a surge-type calving glacier with many tributary glaciers / basins. Some information is available on former positions of the glacier front (Fig. 1). From 1991 till 1997 the glacier surged, leading to a 2 km advance of the glacier front (Mansell et al., 2012). Røthe et al. (2015) made a reconstruction of the Equilibrium Line Altitude (ELA) for the Holocene, derived from a thorough analysis of lake sediments in the catchment of the small glacier Karlbreen in northwest Spitsbergen. Karlbreen is located only about 25 km to the west of Monacobreen, and the ELA reconstruction thus offers a unique possibility to simulate the evolution of Monacobreen through Holocene times.



In this study the following questions will be addressed: (i) Is it possible to simulate the late Holocene evolution of Monacobreen ?; (ii) How does the interaction between surging and calving effect the mass budget of the glacier ? ; and (iii) What does the future evolution of the glacier look like for different scenarios of climate change ?

5 2 Glacier model

Monacobreen is modelled as a stream (flowband) of constant width W and length L , to which 10 tributary glaciers / basins supply mass if the equilibrium line is sufficiently low (Fig. 2). The length is measured along the x -axis, which follows the centerline of the flowband. With a width of 5 km and a length of 40 km, the area of the main stream is about 200 km². Currently the area of the tributary basins is 191 km² (not including Seligerbreen), and since these basins have a higher mean surface elevation than the main stream, it is clear that they make a major contribution to the total mass budget. The number of basins that actually feed the main stream depends on L , of course.

2.1 Basic formulation

The evolution of the glacier system is described by the conservation of mass (or volume, since ice density is considered to be constant). Since a distinction is made between the main stream and tributary glaciers, the governing equation is conveniently written as:

$$\frac{dV}{dt} = F + B_M + \sum_{i=1}^{10} B_i = B_{tot} , \quad (1)$$

where V is the volume of the main stream of Monacobreen, F is the calving flux (< 0), B_M is the surface mass budget of the main stream, and the B_i are the contributions from the tributary glaciers. The total mass budget of the main stream is denoted by B_{tot} . The calculation of the mass fluxes from the tributaries is discussed in section 2.2.

The glacier volume V (of the main stream) is given by WLH_m , where H_m is the mean ice thickness. Differentiating with respect to time yields

$$\frac{dV}{dt} = W \frac{d}{dt} (LH_m) = W \left(H_m \frac{dL}{dt} + L \frac{dH_m}{dt} \right) = B_{tot} . \quad (2)$$

The mean ice thickness is written as (Oerlemans, 2011)

$$H_m = S \frac{\alpha}{1+\nu \bar{s}} L^{1/2} . \quad (3)$$

Here \bar{s} is the mean bed slope over the glacier length, and thus varies in time. S is the "surge function", making it possible to impose a surge cycle. A rapid decrease in S leads to a reduction of the mean ice thickness and consequently an increase in the glacier length to fulfill mass conservation. This technique was successfully applied in the study of Abrahamsbreen referred to earlier. The form of $S(t)$ will be described later. Eq. (3) is based on extensive numerical experimentation with a Shallow Ice Approximation model, including a Weertman type sliding law. For many glaciers the parameter values $\nu = 10$ and $\alpha = 3 \text{ m}^{1/2}$ work well, but the larger glaciers in northern Svalbard apparently flow over beds with relatively low resistance and smaller values of α apply (to be discussed later). Note that in the limit for $\bar{s} \rightarrow 0$ the mean thickness varies with the square root of the glacier length, which is in agreement with the standard analytical theory for plane shearing flow (Vialov, 1958).

After some algebraic manipulation (Oerlemans, 2011), the prognostic equation for glacier length can be written as



$$\frac{dL}{dt} = \frac{B_{tot}}{W(a_1+a_2)} - \frac{a_3}{(a_1+a_2)} \frac{dS}{dt}, \quad (4)$$

where

$$a_1 = \frac{3}{2}H_m; \quad a_2 = -\frac{\nu H_m L}{(1+\nu s)} \frac{\partial \bar{s}}{\partial L}; \quad a_3 = -\frac{H_m L}{s}. \quad (5)$$

The expressions for \bar{s} and $\partial \bar{s} / \partial L$ will be given in section 2.3, where the bed geometry is discussed.

5 2.2 The mass budget

Surface mass balance measurements are not available for Monacobreen, and therefore the same strategy is followed as in the study of Abrahamsenbreen. Based on existing mass balance observations on glaciers in northwest Spitsbergen filed at the World Glacier Monitoring Service (Zürich), the balance rate \dot{b} is taken as a linear function of altitude, i.e.

$$\dot{b} = \beta(h - E), \quad (6)$$

10 where E is the equilibrium-line altitude and β is the balance gradient. From the measurements it appears that a characteristic value is $\beta = 0.0045 \text{ m w.e. m}^{-1}$ (Oerlemans and Van Pelt, 2015). The equilibrium-line altitude is used as the parameter to impose climate change to the glacier model (to be discussed later). The total mass loss or gain of the flowband is found by integrating the balance rate over the glacier length:

$$B_s = \beta W \int_0^L [H(x) + b(x) - E] dx = \beta (H_m + \bar{b} - E) WL, \quad (7)$$

15 where \bar{b} is the mean bed elevation of the glacier (note that this quantity depends on the glacier length).

The tributary glaciers / basins are treated in a simple way, in which the surface geometry is fixed. This is justified because the tributaries have larger slopes and therefore a weaker altitude - mass balance feedback. The tributaries only supply mass to the main stream when they have a positive budget, which is the case when the mean surface elevation is less than E . Each tributary glacier is described as a basin with a tilted trapezoidal shape. The basin has length L_y and width $w(y) = w_0 + qy$,
 20 where y is a local coordinate running from the lowest part of the basin ($y = 0$) to the highest point of the basin ($y = L_y$). The surface elevation is taken as $h(y) = h_0 + sy$, where s is the surface slope. Each of the ten individual basins is thus characterized by five parameters: L_y, w_0, h_0, s, q . Note that the basins can become narrower when going up ($q < 0$) are wider ($q > 0$). The values of the geometric parameters were all estimated from the topographical map referred to in section 1, and are listed in Table 1. The total mass budget B_i of basin i is found to be

$$25 \quad B_i = \beta \int_0^{L_y} (b_0 + sy - E)(w_0 + qy) dy = \quad (8)$$

$$= \beta \left[w_0(b_0 - E)L_y + \frac{1}{2} \{s w_0 + (b_0 - E)q\} L_y^2 + \frac{1}{3} s q L_y^3 \right].$$

The final term in the mass budget is the calving rate. The calving rate is assumed to be proportional to the water depth d , so the calving flux can be written as

$$F = -cdWH_f, \quad (9)$$

30 where H_f is the ice thickness at the glacier front, and c is the 'calving parameter'. The formulation of a calving law has been a controversial issue since a long time. The type of calving law formulated in eq. (9) has been suggested by, among others, Brown et al. (1982), Funk and Röthlisberger, 1989; Pelto and Warren (1991), Björnsson et al. (2000). There are many mechanisms leading to the production of icebergs (for a comprehensive review, see Benn et al., 2007). In recent years



numerical models have been developed that simulate the calving process in great detail (e.g. Krug et al., 2014). Results from such models provide insight into the details of the calving process, but cannot be simply used to formulate a more general calving law for use in large-scale models of tidewater glaciers. In the present study the interest is in the global dynamics of a glacier system and its evolution on larger time scales. It is therefore reasonable to assume that mass loss by calving is
5 generally larger when the glacier front is in deeper water.

The thickness at the glacier front is not explicitly calculated and therefore has to be expressed in the mean ice thickness and/or glacier length. As for Hansbreen, the following parameterization is used

$$H_f = \max\{\kappa H_m; \delta\} \quad , \quad (10)$$

where δ is the ratio of water density to ice density. So according to eq. (10) the ice thickness can never be less than the
10 critical thickness for flotation. The use of eq. (10) allows the model glacier to undergo a smooth transition between a land-based terminus and a calving front.

At Hansbreen, polish scientists have produced the longest series of calving flux measurements for any tidewater glacier in Svalbard (Błaszczuk et al., 2009; Petlicki et al., 2015). There are certain similarities between the calving fronts of Hansbreen and Monacobreen. The water depth around the current location of the calving front is in the same range, and both glaciers
15 exhibit a seasonal fluctuation of the calving front position of comparable magnitude (see also Mansell et al., 2012). There are no systematic observations of the calving flux at Monacobreen that allow to determine a value of c . Therefore in this study the same value is used as found for Hansbreen, namely $c = 1.15 \text{ yr}^{-1}$.

2.3 Geometry of the mean stream

The bed of Monacobreen has never been mapped. Airborne radio-echo sounding in the past has revealed strong internal
20 reflections, and it appeared to be impossible to map the bed of the glacier (Dowdeswell et al., 1984). Until today, the thickness of Monacobreen is unknown. Methods have been developed to estimate ice thickness from the surface topography, with or without information about the surface mass balance distributions (Farinotti et al., 2017). At the present state of the art, these methods do not yet appear to be reliable for the larger glaciers in Spitsbergen. Input data is too uncertain and the condition of near-equilibrium, needed to estimate the balance flux, is not met. The fact that time scales are large and surge
25 behaviour is present, complicates the application of ice-thickness models substantially. In addition there is a large uncertainty about the sliding regime. A few test calculations done by the author revealed that estimated ice thicknesses are much too large for the few glaciers on Spitsbergen for which bed elevation data exist.

However, the surface elevation of Monacobreen is quite smooth and regular (Fig. 3) and it seems unlikely that there are significant overdeepenings or major steps in the bed. For the nearby glaciers Kronebreen and Kongsvegen, a compilation of
30 bedrock data from various sources was published by Hagen and Saetrang (1991), with a further analysis in Melvold and Hagen (1998). Kronebreen descends from the same plateau as Monacobreen, albeit in the other direction. The bed profile of Kronebreen can be represented reasonably well with a function of the form $b_h \exp(-x/\lambda)$, where b_h is the bed height at the glacier head ($x = 0$) and λ is the length scale that determines how fast the bed drops off along the glacier flowline (Van Dongen, 2014). Appropriate values for Kronebreen are $b_h = 1100 \text{ m}$ and $\lambda = 12000 \text{ m}$. By assuming a similarity between
35 the bed profiles of Kronebreen and Monacobreen, and realizing that Monacobreen is slightly longer, the appropriate value for λ would be 15000 m.

In view of these considerations, the following bed profile was chosen for Monacobreen:

$$b(x) = b_a + b_h \exp(-x/\lambda) \quad . \quad (11)$$



The value of b_a (negative for a tidewater glacier) determines the bed height for ($x \rightarrow 0$), and the bed elevation at the head of the glacier now is $b_a + b_h$. The mean bed slope over the length of the glacier, needed in eq. (5), thus becomes

$$\bar{s} = \frac{b_h [1 - \exp(-\frac{L}{\lambda})]}{L}. \quad (12)$$

The change of the mean bed slope with L , also needed in eq. (5), becomes

$$5 \quad \frac{\partial \bar{s}}{\partial L} = -\frac{b_h [1 - \exp(-\frac{L}{\lambda})]}{L^2} + \frac{b_h \exp(-\frac{L}{\lambda})}{\lambda L}. \quad (13)$$

Finally, the mean bed elevation over the glacier length, needed in eq. (7) is

$$\bar{b} = b_a + \frac{b_h \lambda [1 - \exp(-\frac{L}{\lambda})]}{L}. \quad (14)$$

The bathymetry of Liefdefjorden is well known (e.g. Hansen, 2014). The water depth varies considerably, but is mostly between 50 and 150 m. It is therefore appropriate to use $b_a = -150$ m. The resulting bed profile is shown in Fig. 3. Note that with this choice of parameters calving occurs whenever the glacier is longer than 27 km. The mean ice thickness for the present state of the glacier is about 300 m. The corresponding value for α in eq. (3) is $2.05 \text{ m}^{1/2}$. This is a fairly small value compared to the measured value for Hansbreen ($3 \text{ m}^{1/2}$), but larger than that found for Kronebreen ($1.43 \text{ m}^{1/2}$; Van Dongen, 2014).

2.4 Imposing surges

15 Monacobreen surged from 1991 till 1997. The duration of surges of the larger glaciers in Svalbard is rather long, and Monacobreen forms no exception. The velocity field and front positions during the surge have been documented in detail from analysis of a large number of satellite images (Mansell et al., 2012). During the surge the glacier front advanced by about 2 km. In view of the length of the glacier, this is not much. Although there is no proof for this, it is likely that the LIA maximum stand as mapped in 1907 occurred at the end of a surge. This would suggest that the surge cycle of Monacobreen is about 100 years.

In the model the surge function is prescribed as (Oerlemans, 2011):

$$S(t) = 1 - S_0 (t - t_0) e^{-(t-t_0)/t_s}. \quad (14)$$

The surge starts at $t = t_0$, and the characteristic time scale of the surge is denoted by t_s . S_0 determines by how much the mean ice thickness is reduced at the end of the surge.

25 Surges as reproduced in the model are shown in Fig. 4. It appears that the observed amplitude and duration of the surge can be matched well with $S_0 = 0.024 \text{ yr}^{-1}$ and $t_s = 8 \text{ yr}$. A surge cycle of 100 years has been prescribed. The equilibrium-line altitude was constant and set to 619 m, because this produces a glacier length of about 40 km. When a surge begins, the mean ice thickness (and thus surface elevation) immediately starts to decrease. This is a direct consequence of mass conservation, of course. The lower surface leads to a negative net balance that peaks at the end of the surge. The curves for the net balance and mean ice thickness are not identical, as the glacier area also changes (the net balance is the total mass budget divided by the glacier area). The change in the net balance also involves a contribution from the changing calving rate, but for the present geometric set up (the water depth increase only very slightly at the glacier front) this is an insignificant effect. The maximum perturbation of the net balance is only $-0.125 \text{ m w.e. yr}^{-1}$. This is much less than for Abrahamsbreen, where it was found to be $-0.5 \text{ m w.e. yr}^{-1}$ (Oerlemans and Van Pelt, 2015). The difference stems from the fact that the relative surge amplitude (maximum frontal advance divided by glacier length) for Abrahamsbreen is more



than twice that for Monacobreen. In view of the small effect on the net balance, it is likely that the effect of regular surging on the long-term response of Monacobreen to climatic change is limited. This will be investigated shortly.

2.5 Basic sensitivity and response time

According to the map in Hagen et al. (1993), the estimated equilibrium-line altitude in the region of Monacobreen is 500 to 600 m a.s.l., with a tendency to lower values when going in northwesterly direction. The estimate is based on an assumption of balance, i.e. a situation in which the glaciers would be in equilibrium. This is currently not the case and the equilibrium line over the past decades has certainly been higher. In the model the value of E is taken the same for the entire domain, except for basins 1, 2 and 3, where E is perturbed by -100, -100, and -50 m, respectively. These perturbations are applied in all calculations presented in this paper.

The evolution of Monacobreen for stepwise forcing of the equilibrium line is shown in Fig. 5. As can be expected in view of the very small slope, it turns out that the climate sensitivity of the glacier is very large. Changing E from 800 to 600 m makes the glacier grow by 23 km. Bringing back the equilibrium line to 600 m (in two steps) does not reveal a sign of hysteresis (as would occur when there would be an overdeepening in the bed). The adjustment to a changing climate apparently takes a long time: the e-folding response time is about 350 years.

The corresponding components of the mass budget are shown in Fig. 5. To facilitate a comparison, all components are expressed as a specific balance. The important role played by the tributary glaciers / basins becomes clear immediately. Only at $t = 500$ yr, when E drops instantaneously by 200 m, does the main stream have a positive balance. This does not last very long, however, because the increasing glacier length soon leads to a much larger ablation zone. When the glacier length is of the order of 40 km, as it is today, the negative net surface balance of the main stream and the calving flux contribute roughly equally to the compensation of the net input from the tributaries.

3 Climatic forcing

A simulation of the Holocene evolution of Monacobreen requires an appropriate climatic forcing function. Fortunately, a ELA history for a small valley glacier on Mitrahelvøya, which is only 25 km west of the central part of Monacobreen, has been reconstructed from lake sediments (Røthe et al., 2014). This glacier, Karlbreen, currently has an area of about 2 km² and the glacier head is at about 500 m a.s.l. This is an important height because it puts a lower limit on the ELA in times that there was no glacial activity. The glacier drains through a series of three lakes and an extensive sediment analysis has provided a full history of glacial activity. By using former glacier stands, Røthe et al. (2014) were able to convert sediment parameters to ELA values, assuming an equilibrium between glacier size and ELA. According to Røthe et al. (2014), there was very little glacial activity during the period 9200 to 3500 yr BP, implying the the equilibrium line was mostly about 500 m a.s.l. After the Holocene Climatic Optimum there is a long-term trend towards lower values of the ELA, with significant fluctuations superposed on this. Since a glacier like Karlbreen probably has a response of the order of 20 to 30 years, the reconstruction is bound to be less accurate for shorter time scales. Therefore the reconstruction for Karlbreen is combined with ELA's estimated from meteorological observations at Longyearbyen / Svalbard airport since 1899 (Førland et al., 2011). It should be noted that there is a distinct west-east gradient in the ELA in northwest Spitsbergen (Hagen et al., 1993). The ELA rises in eastward direction, mainly due to lower precipitation rates. Therefore, the *absolute* reconstructed ELA values cannot be used to force the model for Monacobreen, so the ELA perturbation E_R relative to a reference value E_0 is used. The ELA is now formulated as

$$\text{for } t < 1899: E(t) = E_0 + E_R(t) . \quad (15a)$$



$$\text{for } t \geq 1899: E(t) = E_1 + E_M(t) . \quad (15b)$$

Here $E_M(t)$ is the ELA perturbation obtained from the meteorological data, as described in Oerlemans and Van Pelt (2015).

The relation between the ELA and temperature / precipitation is based on calculations with an energy balance model, giving sensitivities of $\partial E / \partial T = 35 \text{ m K}^{-1}$ and $\partial E / \partial P = -2.25 \text{ m \%}^{-1}$. Here T and P are perturbations of the annual mean temperature and precipitation.

The constants E_0 and E_1 need not necessarily be the same, because it is unknown how precisely the meteorological observations connect to the past. These constants will therefore be used as tuning parameters.

4 Simulation of the Holocene evolution of Monacobreen

The ELA reconstruction from the Karlbreen basin is available from the year 2155 BC, but the model integration starts a bit earlier to have an equilibrated state at this time. For the final outcome the precise choice is not important, because the response time of the glacier is much shorter than the period of integration. Surging is included, and the duration of the surge cycle is set to 100 yr. The strategy is simple: trying to adjust the values of E_0 and E_1 until the LIA maximum stand ($L = 43.3$ km) and the 1997 maximum front position at the end of the surge ($L = 40.7$ km) are reproduced. This turned out to be the case for $E_0 = 605 \text{ m a.s.l.}$ and $E_1 = 665 \text{ m a.s.l.}$, which are plausible values. There appeared to be no need to adjust the calving parameter.

The corresponding evolution of the glacier length is shown in Fig. 6. Due to declining summer insolation, at the end of the Holocene Climatic Optimum the arctic climate cools and the equilibrium line drops. For Monacobreen the ELA is then around 850 m and the length of the glacier is about 15 km. From 1700 BC the ELA decreases markedly, the glacier grows to a size of about 30 km and becomes a tidewater glacier. During a few centuries BC, the ELA lingers around a value of about 700 m, until it drops by another 100 m in the first century AD. In this range of ELA values Monacobreen is quite sensitive, and the 100 m drop in the ELA is sufficient to make the glacier grow to its current size. The lowest ELA values for the entire period are during the 19th century and this then leads to a maximum glacier stand around 1900 (in combination with the surge). The rise of the ELA during the 20th century leads to a 3.5 km retreat of the glacier front until the last surge start in 1991. This surge coincides with a sharp increase in the ELA of another 100 m, and as a consequence the retreat of the glacier front after the surge is almost twice as fast as after the previous surge. It is noteworthy that the simulated position of the glacier front in 2016 matches the observed position accurately without any further tuning. Apparently this result can be obtained with a calving parameter that is constant in time. This is in agreement with the analysis of Mansell et al. (2012), who did not find significant fluctuations in the calving rate during the surge. Altogether, the simulated evolution of Monacobreen during the Holocene is in very good agreement with the observational evidence. A great deal of this result is probably on the account of the realistic ELA reconstruction from the Karlbreen basin (Røthe et al., 2014).

The components of the mass budget corresponding to the model integration of Fig. 6 are shown in Fig. 7. For reference the glacier length is also shown. A distinction is made between the total contribution from the tributaries, the surface balance of the main stream and the calving flux. All components are shown as a specific balance, i.e. expressed as a specific net loss or gain averaged over the area of the main stream. Apparently the contribution from the tributaries is always positive, and the surface balance of the main stream is always negative. Since these two components are entirely determined by changes in the ELA, which are always the same over the entire domain, it is not surprising that the fluctuations are highly correlated (note that the area of the main stream varies a lot). Around 500 yr BC Monacobreen becomes a tidewater glacier and the calving flux gradually becomes more important. During the past 1000 years the mass loss by calving is of the same order as the surface



balance of the main stream. However, after the 1991-1997 surge the surface balance of the main stream has become much more negative, and represents a greater loss than the calving. This is clearly due to the strong increase in the ELA.

Fig. 8. Shows the results of some sensitivity tests. First of all surging was switched off. Because the surge amplitude is quite small (see discussion in section 2.4), it is not surprising that the effect of surging on the long-term evolution of Monacobreen is limited. In the absence of surging the mean glacier length (e.g. averaged as a 100-yr running mean value) is slightly larger, the difference typically being 0.5 km. In a second test calving was switched off ($c = 0$). This has a profound effect on the late-Holocene evolution of the glacier. The model predicts that without mass loss by calving the glacier would at present be 15 km longer.

It is also interesting to switch off some of the tributary glaciers. This reveals that the tributaries further downstream make a relatively small contribution. The largest contributions come from basins 5 and 6, which have a higher mean surface elevation and a large area (notably basin 6). When the input from basins 5 and 6 is switched off, the present glacier length would be only 30 km.

5 Future evolution of Monacobreen

Recent trends and future climate change in Svalbard has been examined in detail by Fjørland et al. (2011). There is broad agreement between temperature trends obtained by downscaling results from global climate models (forced with greenhouse gas emissions) and observations at Svalbard Airport for the period 1912–2010. Projections for the Svalbard region indicate a future warming rate up to year 2100 three times larger than the observed rate during the past 100 years. For precipitation, the long-term observational series show a modest increase over the past 100 years and projections indicate a further increase up to year 2100. In the present study the projected changes in temperature and precipitation for northwest Spitsbergen will be used to estimate the future trend in the ELA.

For the B2 emission scenario (IPCC, 2013), the rate at which annual temperature and precipitation increases in the ensemble-mean projection is fairly linear until about 2090 and levels off somewhat afterwards (Fjørland et al., 2011). Combining the mid-B2 annual temperature and precipitation trends with the ELA sensitivities discussed in section 3 yields $dE/dt = 1.86$ m/yr. Against this reference the possible future evolution of Monacobreen was studied by imposing values of dE/dt of 0, 2 and 4 m/yr. It should be noted that these values have also been used for glaciers in other parts of the world (e.g. in the Alps; Oerlemans et al., 2017). Although warming is larger in the polar regions (the 'polar amplification'), this is not so much reflected in the rise of the equilibrium line. The reason is that summer temperatures increase much less than annual mean temperatures. In the calculation of the ELA sensitivities this has been taken into account.

Obviously, the outcome depends on the choice of the reference period. It is unclear to what extent the very high ELA values since 2000 represent an expression of natural variability on the decadal time scale, or are a direct response to greenhouse-gas induced warming. To deal with this uncertainty, two 30-yr reference periods were used to define the ELA perturbation associated with the projected climate change: (i) 1987-2016, i.e. the most recent 30-yr period; and (ii) 1961-1990 as the last official period to define the climatology. The resulting six projections of glacier length are shown in Fig. 9a. The integrations are extended until 2200, and the ELA-perturbation is kept fixed after 2100. The curves immediately make clear that much of the response to 21st century warming will come after 2100.

For reference period (ii) and no climate change ($dE/dt = 0$), Monacobreen would hardly retreat. Note that this scenario actually implies that ELA values return to significantly lower values than observed over the last two decades. In contrast, for reference period (i) and no climate change, at 2100 the glacier front would have retreated by 3.5 km.

For the strong-warming scenario with $dE/dt = 4$ m/yr and reference period (i), the model predicts a glacier retreat of about 9 km by the year 2100. At this point the glacier would be grossly out of balance, since the ELA is then at 1038 m a.s.l.,



which is above most of the accumulation basin. In 2100 the volume of Monacobreen would be about 60% of the present-day volume (Fig. 9b).

If the Paris-agreement would become reality, the mid-B2 scenario with $dE/dt = 2$ m/yr is perhaps the most likely one. In this case the front of Monacobreen would retreat by 3.5 to 5.5 km in the coming 80 years, depending on the choice of
5 reference period. The glacier volume would have been reduced by 20 to 30 % with respect to the current volume.

6 Discussion

In this paper it has been demonstrated that the conceptual simplicity of the MGM makes it possible to study the response of a large tidewater glacier to climate change in a transparent way. Calibration turned out to be a straightforward procedure, in which three characteristic glacier front positions could be reproduced accurately (LIA maximum stand, front position at the
10 end of the recent surge, present-day front position). Here the quality of the reconstructed ELA history from Røthe et al. (2014) certainly plays an important role. The approach of defining a main stream that is fed by tributary glaciers / basins seems to work well. The tributary basins were included in a passive way. In fact, the basins were assumed to have a fixed
15 geometry and to be in balance with the prevailing ELA. This should work well as long as the characteristic time scales of the basins are shorter than that of the main stream (perhaps for Louetbreen this is not quite the case). In principle all individual
basins can be modelled with a MGM as well, implying the introduction of a response time and the local height - mass
balance feedback. However, for the present study this was not considered appropriate given the little information available
for these basins.

A significant result from this study is that surging has a limited effect on the long-term evolution of Monacobreen. The relative surge amplitude A_s , loosely defined as the maximum advance divided by the glacier length, is quite small (≈ 0.05).
20 A_s determines to a large extent by how much the mean surface elevation drops. The combined effect of a lower surface elevation and a larger area determines the mass-budget perturbation implied by the surge. It was found that for Monacobreen this perturbation amounts to -0.16 m w.e. yr^{-1} (when expressed as a change in the net balance rate of the main stream, see Fig. 4). It is interesting to compare these numbers with those of Abrahamsenbreen (Oerlemans and Van Pelt, 2015). For
Abrahamsenbreen the surge amplitude is 0.14, and the perturbation of the mass budget about -0.5 m w.e. yr^{-1} .

The largest uncertainty in this study probably stems from the choice of bed profile (Fig. 3). Although the surface of Monacobreen along the central flowband is smooth with a gentle and fairly constant slope, the bed longitudinal bed profile could be more or less concave than actually assumed. Some test calculations were done to see the effect of such a change (keeping the highest point of the bed as well as the depth at the current front position equal). A less concave bed implies a
higher mean surface elevation and a smaller calving flux when the glacier shortens. However, when the model is recalibrated
30 to give the observed mean surface elevation (by adjusting the value of α) and the correct glacier stands referred to earlier (by adjusting the values of E_0 and E_1) the glacier evolution is quite similar. With respect to projected changes in glacier length (Fig. 9), it appears that the major uncertainty comes from the choice of climate change scenario, not from uncertainty in the model parameters.

The MGM has very simple dynamics: there is no spatial resolution and the mechanics are contained in a relation between length, mean ice thickness and mean bed slope, with simple formulations of the calving and surging processes. These formulations do not shed further light on the *nature* of the calving and surging processes, but the effects on the mass budget, and thus on the long term evolution of the glacier, are dealt with. At this point one may ask whether it would be possible to study the Monacobreen glacier system with a 3-dimensional higher order model and make a comparison with the simple



approach taken here.. Modelling the main stream would probably be feasible, but to deal with all the tributaries would require a large amount of data on the bed geometry which are not available and thus would have to be generated indirectly. Generating the surge cycle in a higher-order model, involving a coupling of ice mechanics and glacier hydrology, is another major difficulty to deal with. Perhaps at the present state of the art, it would be more realistic to strive for a hybrid model, in
5 which a comprehensive model for the main stream is combined with MGM's for the tributary glaciers / basins. However, one should not forget that on longer time scales glacier mechanics are always slaved by the mass budget, although there may be subtle interactions (notably concerning the calving process).

10 Acknowledgements

I am grateful to Torgeir Opeland Røthe (University of Bergen) for making the ELA-reconstruction data available, and to Øyvind Nordli (MET Norway) for supplying meteorological data for Longyearbyen / Svalbard airport. This study has been sponsored by the Netherlands Earth System Science Centre (Utrecht, The Netherlands).

15

References

- Benn, D. I., Hulton, N. R. J., Mottram, R.H.: 'Calving laws', sliding laws' and the stability of tidewater glaciers, *Ann. Glaciol.*, 46, 123-130, 2007.
- Blaszczyk M., Jania, J. A., and Hagen, J. O.: Tidewater glaciers of Svalbard: Recent changes and estimates of calving fluxes,
20 *Polish Polar Research*, 30 (2), 85–142, 2009.
- Björnsson, H.: Scales and rates of glacial sediment removal: a 20 km long, 300 m deep trench created beneath Bredamerkurjökull during the Little Ice Age, *Ann. Glaciol.*, 22, 141–146, 1996.
- Brown, C. S., Meier, M. F. and Post, A.: Calving speed of Alaska tidewater glaciers with applications to the Columbia Glacier, Alaska, U. S. Geol. Surv. Prof. Pap. 1258-C, 13 pp., 1982.
- 25 Dowdeswell, J. A., Drewry, D. J., Liestel, O. and Orheim, O.: Radio-echo sounding of Spitsbergen glaciers: problems in the interpretation of layer and bottom returns, *J. Glaciol.*, 30 (104), 16-21, 1984.
- Farinotti, D., and many others: How accurate are estimates of glacier thickness? Results from ITMIX, the Ice Thickness Models Intercomparison eXperiment, *The Cryosphere*, 11, 949-970, doi: 10.5194/tc-11-949-2017, 2017.
- Førland, E. J., Benestad, R., Hanssen-Baur, I., Haugen, J. E. and Skaugen, T. E.: Temperature and precipitation development
30 at Svalbard 1900-2100, *Adv. Meteorol.*, 2011, doi: 10.1155/2011/893790. 2011.
- Funk, M., and Röthlisberger, H.: Forecasting the effects of a planned reservoir which will partially flood the tongue of Unteraargletscher in Switzerland, *Ann. Glaciol.*, 13, 76-81, 1989.
- Hagen J. O., Liestøl O., Roland E. and Jørgensen T.: Glacier atlas of Svalbard and Jan Mayen, *Norsk Polarinstitutt Medd. nr.* 129, 1993.



- Hagen J. O., Saetrang A.: Radio-echo soundings of sub-polar glaciers with low-frequency radar, *Polar Res.*, 9 (1), 99-107, doi: 10.3402/polar.v9i1.6782, 1991.
- Hansen, T.: Late Weichselian and Holocene sedimentary processes and glacier dynamics in Woodfjorden, Bockfjorden and Liefdefjorden, North Spitsbergen, Master thesis, The Arctic University of Norway, 2014.
- 5 Huss, M. and Hock, R.: A new model for global glacier change and sea-level rise, *Front. Earth Sci.*, 3, doi:10.3389/feart.2015.00054, 2015.
- Huybrechts, P., De Nooze, P. and Declerq, H.: Numerical modelling of Glacier d'Argentière and its historic front variations. In Oerlemans, J., ed. *Glacier fluctuations and climatic change*. Dordrecht, etc., Kluwer Academic Publishers, 373-389, 1989.
- 10 IPCC, 2013: *Climate Change 2013: The Physical Science Basis. Contribution of Working Group I to the Fifth Assessment Report of the Intergovernmental Panel on Climate Change* [Stocker, T.F., D. Qin, G.-K. Plattner, M. Tignor, S.K. Allen, J. Boschung, A. Nauels, Y. Xia, V. Bex and P.M. Midgley (eds.)]. Cambridge University Press, Cambridge, United Kingdom and New York, NY, USA, 1535 pp, doi:10.1017/CBO9781107415324.
- Jouvet G., Huss, M., Blatter, H., Picasso, M., and Rappaz, J.: Numerical simulation of Rhonegletscher from 1874 to 2100, *J. Comput. Phys.*, 17, 6426-6439, doi:10.1016/j.jcp.2009.05.033, 2009.
- 15 Krug, J., Weiss, J., Gagliardini, O. and Durand, G.: Combining damage and fracture mechanics to model calving, *The Cryosphere*, 8, 2101-2117, 2014.
- Kruss, P.: Terminus response of Lewis Glacier, Mount Kenya, Kenya, to sinusoidal net-balance forcing, *J. Glaciol.*, 30 (105), 212-217, 1984.
- 20 Leclerq, P. W., Oerlemans, J., Basagic, H. J., Bushueva, I., Cook, A. J. and Le Bris, R.: A data set of worldwide glacier fluctuations, *The Cryosphere*, 8, 659-672, doi: 10.5194/tc-8-659-2014, 2014.
- Mansell, D., Luckman, A. and Murray, T.: Dynamics of todewater surge-type glaciers in northwest Svalbard, *J. Glaciol.*, 58, 110-118, doi: 10.3189/2012JoG11J058, 2012.
- Martin-Español, A., Bamber, J. L. and Zammit-Mangion A.: Constraining the mass balance of East Antarctica, *Geophys. Res. Lett.*, 44, 4168-4175, doi:[10.1002/2017GL072937](https://doi.org/10.1002/2017GL072937), 2017.
- 25 Mjelvold, K. and Hagen, J. O.: Evolution of a surge-type glacier in its quiescent phase: Kongsvegen, Spitsbergen, 1964-95, *J. Glaciol.* 44 (147), 394-404, 1998.
- Nick, F. M., Van der Kwast, J. and J. Oerlemans, J.: Simulation of the evolution of Breidamerkurjökull in the late Holocene, *J. Geophys. Res.*, 112, B01103, doi:10.1029/2006JB004358, 2007.
- 30 Oerlemans, J.: A flowline model for Nigardsbreen, Norway: projection of future glacier length based on dynamic calibration with the historic record, *Ann. Glaciol.*, 24, 382-389, 1997.
- Oerlemans, J.: *Minimal Glacier Models*. Second edition. Igitur, Utrecht University, ISBN 978-90-6701-022-1, 2011.



- Oerlemans, J., Haag, M. and Keller, F.: Slowing down the retreat of the Morteratsch glacier, Switzerland, by artificially produced summer snow: a feasibility study, *Climatic Change*, 145, 189-203, doi 10.1007/s10584-017-2102-1, 2017.
- J Oerlemans, J., Jania, J. and Kolondra, L.: Application of a minimal glacier model to Hansbreen, Svalbard, *The Cryosphere* 5, 1-11. Doi: 10.5194/tc-5-1-2011, 2011.
- 5 Oerlemans, J. and Van Pelt, W. J. J.: A model study of Abrahamsenbreen, a surging glacier in northern Spitsbergen, *The Cryosphere* 9, 767-779, doi: 10.5194/tc-9-767-2015, 2015.
- Oerlemans, J. and 10 others: Modelling the response of glaciers to climate warming, *Climate Dyn.*, 14(4), 267-274, 1998.
- Pelto, M. S., and Warren, C. R.: Relationship between tidewater glacier calving velocity and water depth at the calving front, *Ann. Glaciol.*, 15, 115-118, 1991.
- 10 Petlicki, M., Cieply, M., Jania, J. A., Promisnka, A. and Kinnard, C.: Calving of tidewater glacier driven by melting at the grounding line, *J. Glaciol.*, 61, 851-862, doi: 10.3189/2015JoG15J062, 2015.
- Radić, V., Bliss, A., Beedlow, A. C., Hock, R., Miles, E., and Cogley, J. G.: Regional and global projections of twenty-first century glacier mass changes in response to climate scenarios from global climate models. *Clim. Dyn.* 42, 37-58. doi: 10.1007/s00382-013-1719-7, 2014.
- 15 Røthe, T. O., Bakke, J., Vasskog, K., Gjerde, M., D'Andrea W. J., and Bradley. R. S.: Arctic Holocene glacier fluctuations reconstructed from lake sediments at Mitrahalyvøya, Spitsbergen, *Quat. Sci. Rev.*, 109, 111-125, doi: [org/10.1016/j.quasscirev.2014.11.017](https://doi.org/10.1016/j.quasscirev.2014.11.017), 2015.
- Schäfer, M., Möller, M., Zwinger, T., and Moore, J. C.: Dynamic modelling of future glacier changes: Mass-balance/elevation feedback in projections for the Vestfonna ice cap, Nordaustlandet, Svalbard, *J. Glaciol.*, 61, 1121-1136,
20 doi:10.3189/2015JoG14J184, 2015.
- Van den Broeke, M. R., Enderlin, E. M., Howat, I. M., Kuipers Munneke, P., Noël, B. P. Y., van de Berg, W. J., van Meijgaard, E., and Wouters, B.: On the recent contribution of the Greenland ice sheet to sea level change, *The Cryosphere*, 10, 1933-1946, <https://doi.org/10.5194/tc-10-1933-2016>, 2016.
- Van Dongen, E.: Application of a minimal model to Kongsvegen and Kronebreen. Thesis, IMAU, Utrecht University, 2014.
- 25 Vialov, S.S.: Regularities of glacial shields movement and the theory of plastic viscous flow, *Int. Assoc. Hydrolog. Sci. Publi.*, 47, 266-275, 1958.
- Zekollari, H., Huybrechts, Ph., Fürst, J., Rybak, J., and Eisen, O.: Calibration of a higher-order 3-D ice-flow model of the Morteratsch glacier complex, Engadin, Switzerland, *Annals of Glaciol.*, 54, 343-351, doi: 10.3189/2013AoG63A434), 2013.
- Zekollari, H., Huybrechts, P., Noël, B., Van de Berg, W. J., and Van den Broeke, M. R.: Sensitivity, stability and future
30 evolution of the world's northernmost ice cap, Hans Tausen Iskappe (Greenland), *The Cryosphere*, 11, 805-825, <https://doi.org/10.5194/tc-11-805-2017>, 2017.
- Zemp, M., and 38 others: Historically unprecedented global glacier decline in the early 21st century, *J. Glaciol.*, 61, 754-761, doi: 10.3189/2015JoG15J017, 2015.



5

10

basin	L_y (m)	w_0 (m)	b_0 (m)	s	q (m)
T1	7000	2200	50	0.14	-1.00
T2	3000	4800	200	0.23	0.0
T3	8500	3000	300	0.065	0.18
T4	3200	1500	550	0.11	0.71
T5	4700	3800	800	0.085	0.54
T6	4300	7500	900	0.11	-0.65
T7	4700	1600	650	0.095	-0.12
T8	7600	1800	500	0.078	0.82
T9	5700	4300	450	0.080	0.70
T10	3800	800	220	0.2	0.54

15

Table 1. Geometrical characteristics of the tributary basins of Monacobreen. Basin numbers as indicated in Fig. 2.

20

25

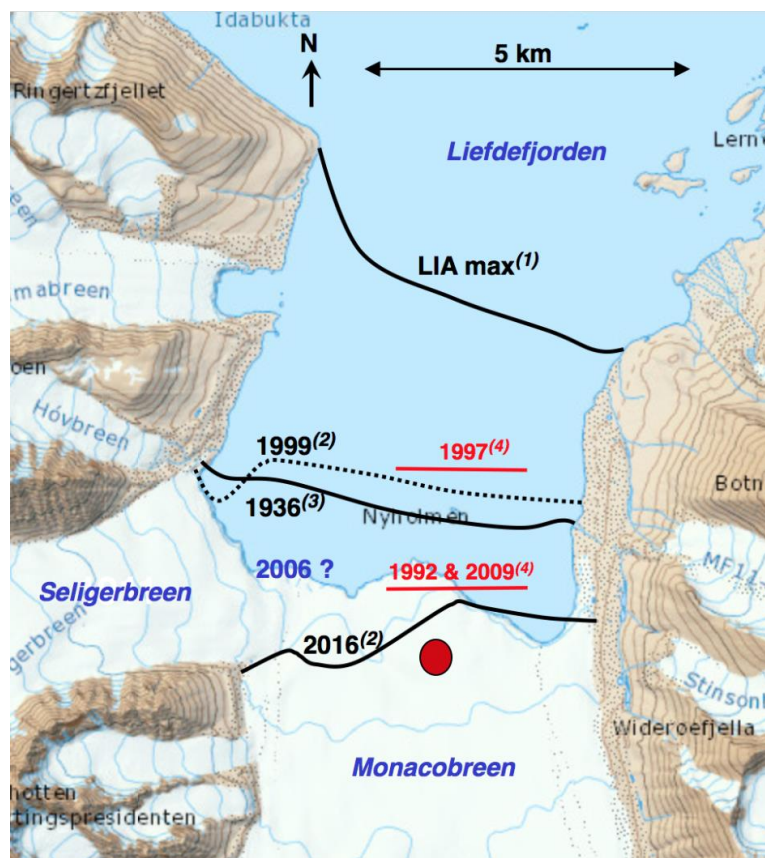


Figure 1. Front positions of Monacobreen in different years, drawn on a topographic map of the Norsk Polatinstiutt (<http://toposvalbard.npolar.no>). The Little Ice Age maximum stand occurred around 1900 (Martin-Moreno et al., 2017), the 1999 and 2016 positions are from Landsat images (Pelto, 2017). The maximum front position related to the surge was in 1997 (Mansell et al., 2012). The 1992 position is just prior to the surge. In 2009 the glacier front had retreated back to this location.

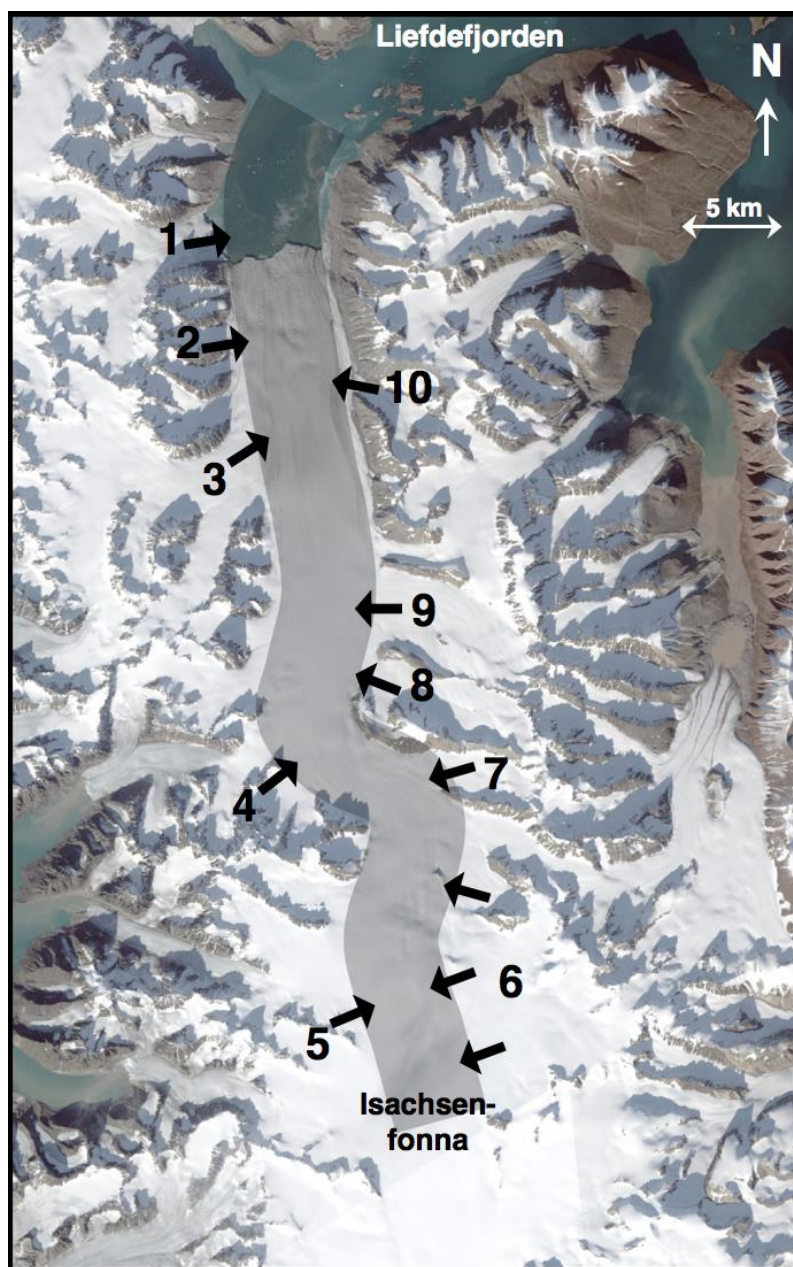


Figure 2. The 43 km long and 5 km wide flowband (grey) used to model Monacobreen, shown as an overlay on a Landsat image (©Norsk 5 Polarinstitut). The tributary glaciers / basins are numbered 1 to 10, and the corresponding geometric properties are listed in Table 1.

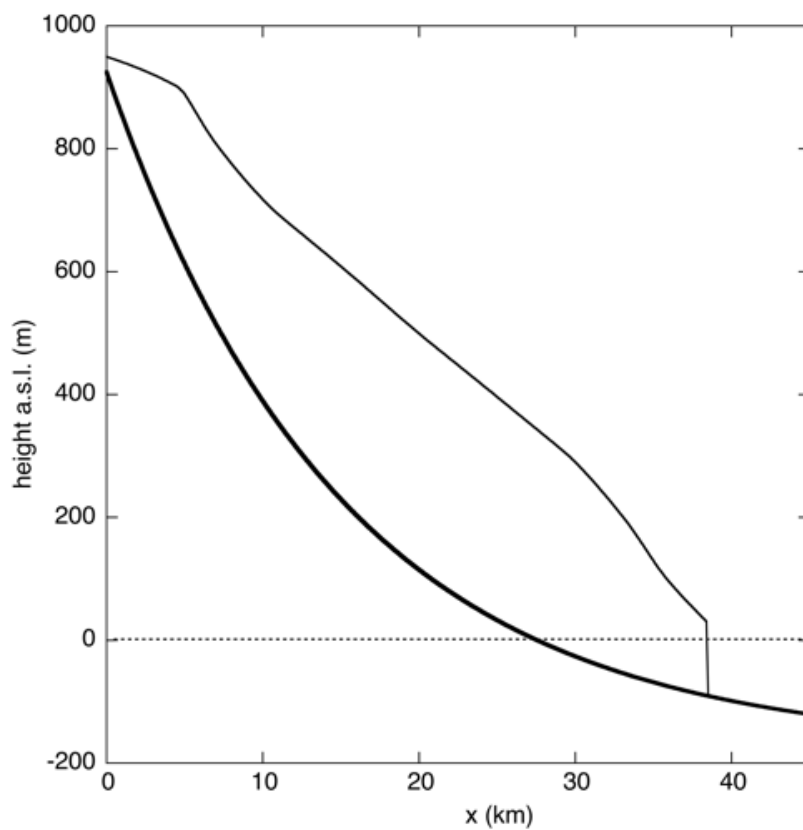


Figure 3. Upper curve: glacier surface elevation of Monacobreen along the flowband according to the topographic map (<http://toposvalbard.npolar.no>). Lower curve: the bed profile as used in the model.

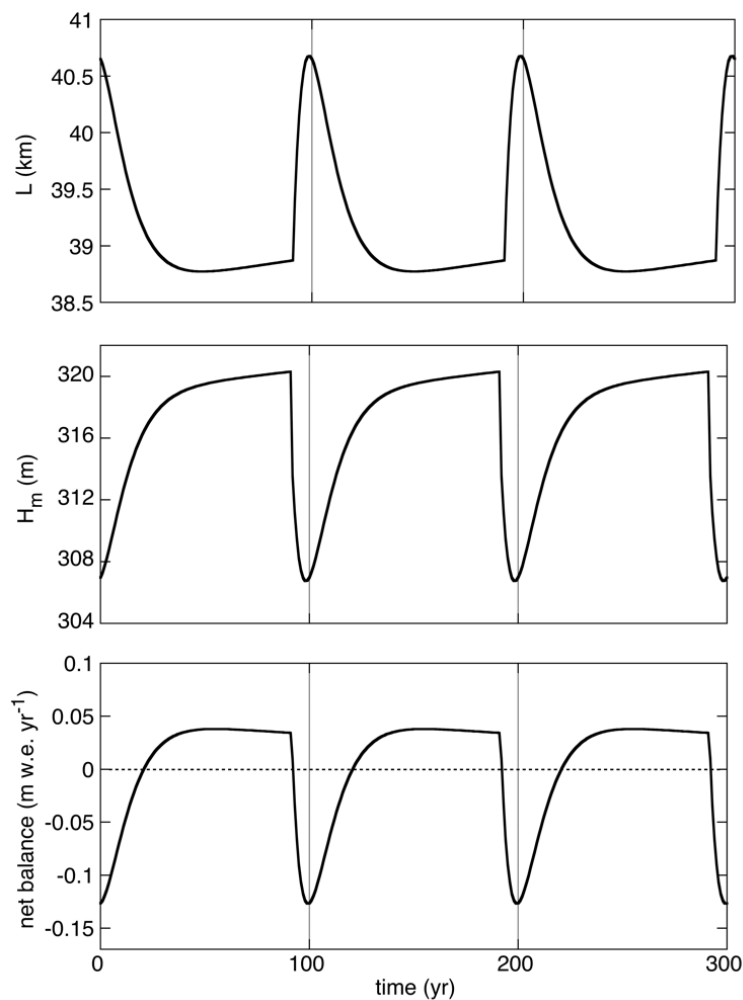


Figure 4. Illustration of the modelled surge cycle, as characterized by glacier length (upper panel), mean ice thickness (middle) and net
5 balance (lower). The surge cycle has been set to 100 years.

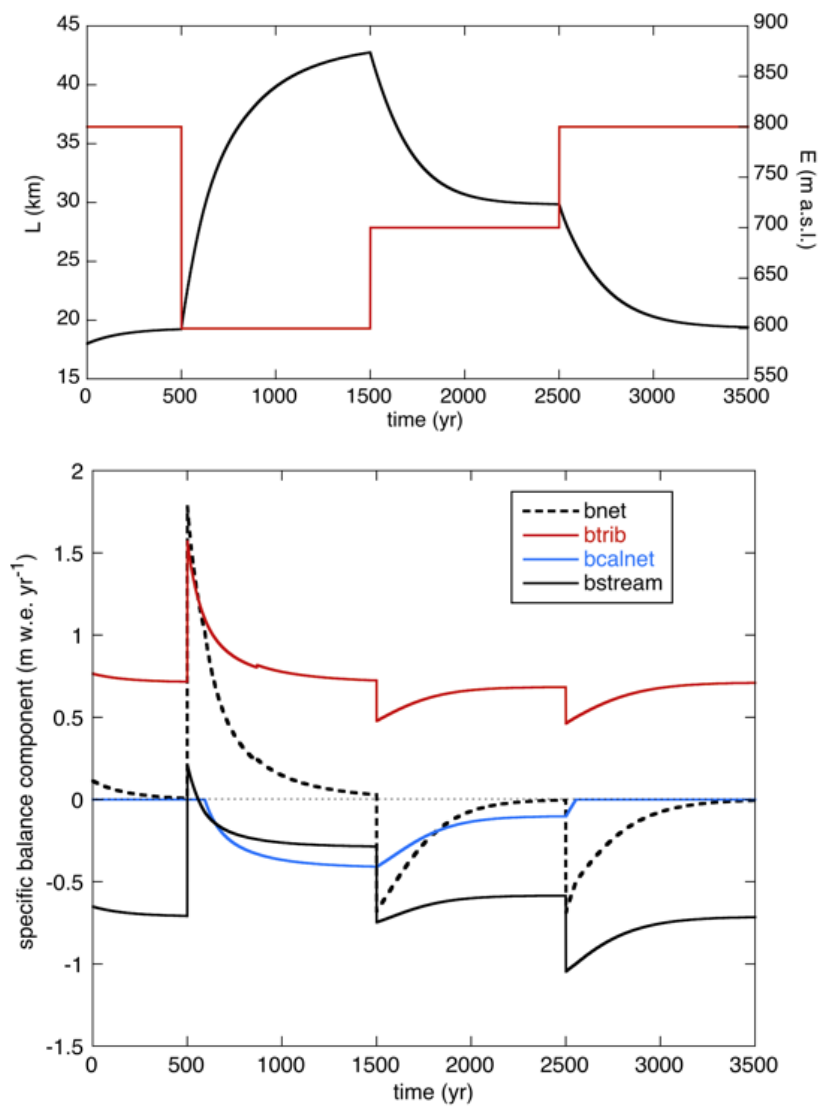


Figure 5. Upper panel: Evolution of glaciers length L (black) for stepwise changes in the equilibrium-line altitude E (in red). Lower panel:
5 The corresponding components of the mass budget.

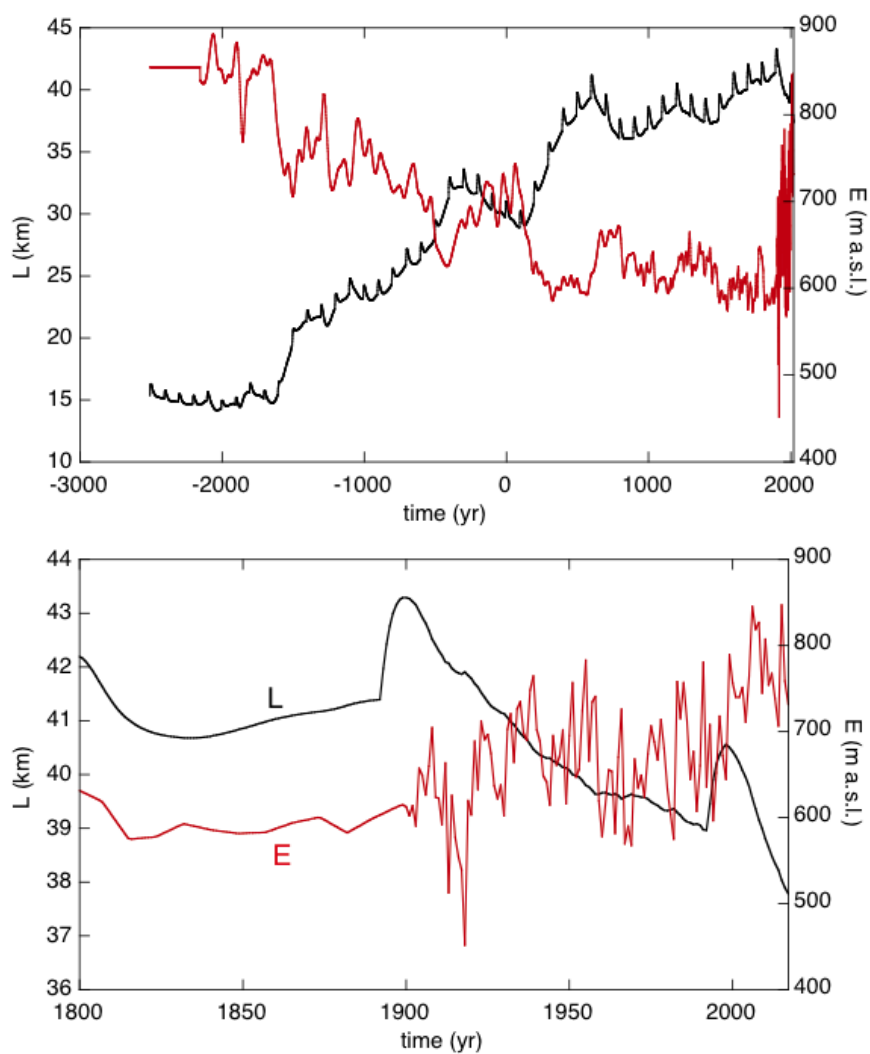


Figure 6. Upper panel: Evolution of glaciers length L (black) for stepwise changes in the equilibrium-line altitude E (in red). Lower panel:
5 close-up of the period 1800 - 2016.

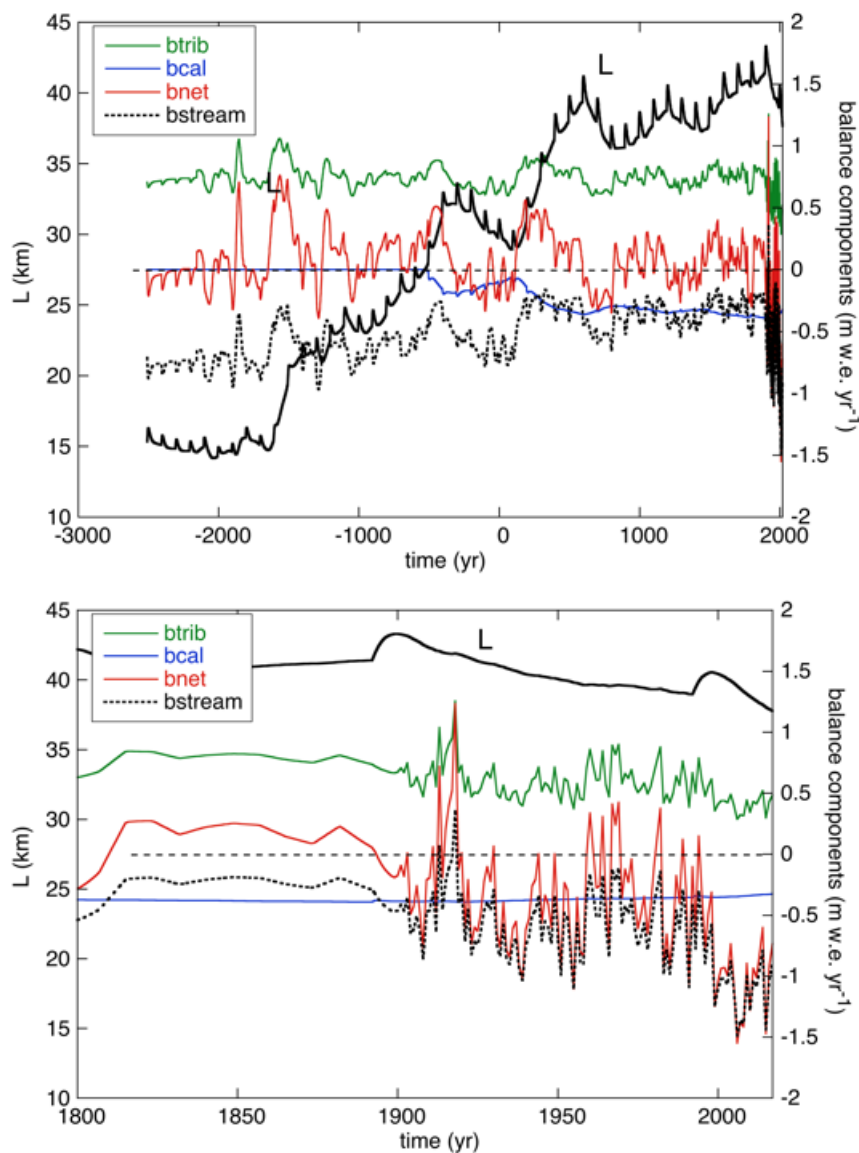


Figure 7. The components of the mass budget corresponding to the simulation shown in Fig. 6, expressed as a specific balance rate.

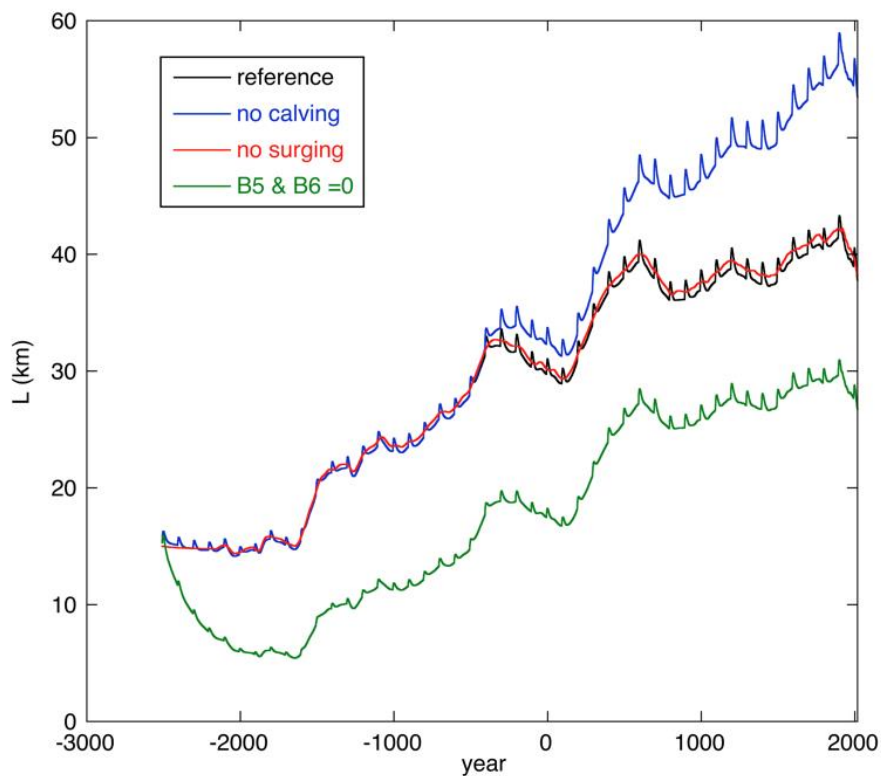


Figure 8. Glacier length resulting from some sensitivity tests. The black curve shows the reference run (identical to the glacier length in 5 Fig. 6).

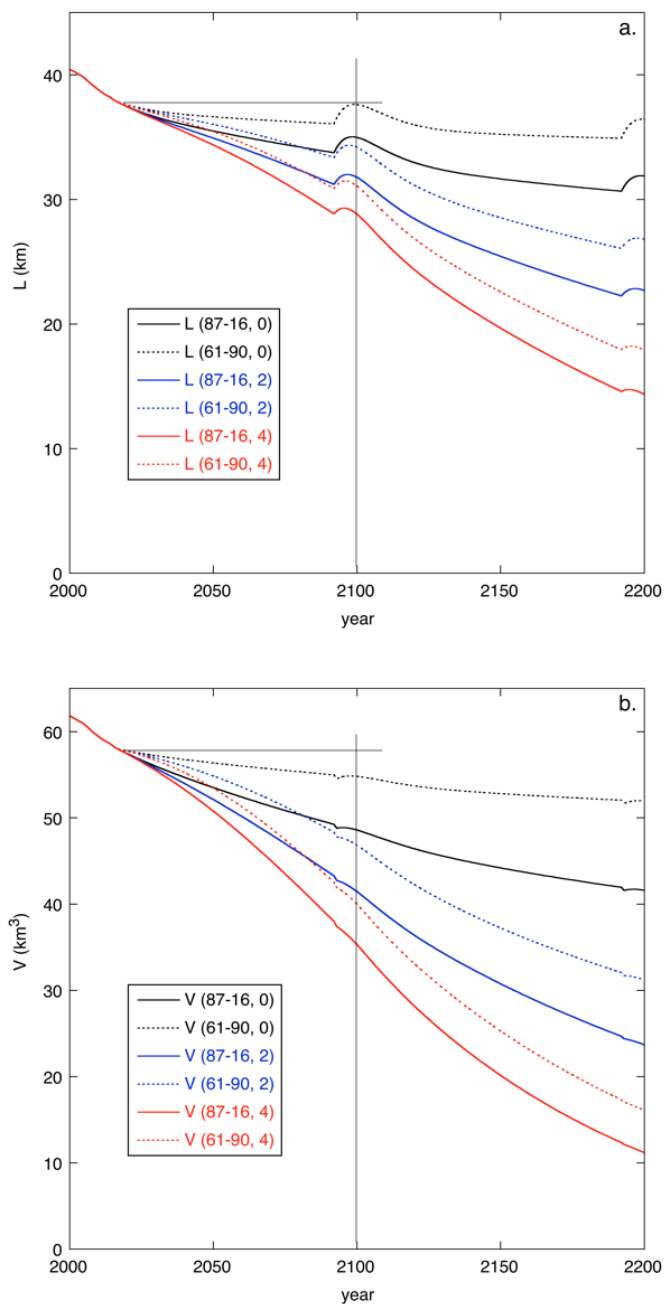


Figure 9. Projections of glacier length (a) and volume (b) for different climate change scenarios. The labels refer to the ELA reference period (either 1961-1990 or 1987-2016) and the rise of the ELA per year during the 21st century (in m/yr).